Modification of shock wave diffraction by pulse gas discharge.

V.P. Fokeev, Yu.I. Grin, V.A. Levin

Institute of mechanics of Moscow State University, 1 Michurinsky pr., 119192 Moscow, Russia
vfokeev@imec.msu.ru

Abstract. The experimental shock tube research dedicated to effects of a pulse gas discharge in air at initial pressure of 20Torr on interaction of a shock wave (M = 2.2-2.5) with a cone of 24˚ half-apex angle and 40mm base diameter. The pulse discharge of 0.3-2.6ms duration was initiated between electrodes located on the cone apex and near the cone back face. Evolution of the disturbed part of the incident shock above discharge region was observed. The formation of a three-shock configuration is revealed at exit from the gas discharge area. The configuration size essentially exceeds Mach configuration on the cone in the discharge absence.

Introduction

Among a number of phenomena connected with the elaboration of pulse detonation engine, both the shock wave diffraction and the plasma-assisted combustion remain topical. In that way the study of pulse gas discharge effect on nonstationary shock waves interaction is advantageous, and in this connection the problem of interaction of shock waves with the bodies of different shapes in presence of neighboring energy deposition region (gas discharge) is also topical.

The given paper is devoted to effect of a pulse gas discharge on the non-stationary shock wave diffraction at shock – cone interaction. The research in effects of plasma formation on the interaction of a shock wave with obstacles is a part of the extensive program of study of gas-dynamic flow control assisted by a gas discharge [1, 2]. The effects of the gas discharge on shock interaction is investigated in many works (see references in [3-5], but in general for stationary shock configuration. Here the problem is illustrated on Figure1, where the shock wave SW moves with velocity **Vs** from left to right. The gas discharge with power supply **Ec** (capacity **C**), and resistance **Rd** in an external electric circuit is charged between cathode **A** and anode **B** (distance **d**). This allows to form the discharge in narrow area (near upper part) near the cone. The discharge starts when the shock is on some distance **L** from a cone, that is the discharge exists during time $\mathbf{t_0=L/Vs}$.

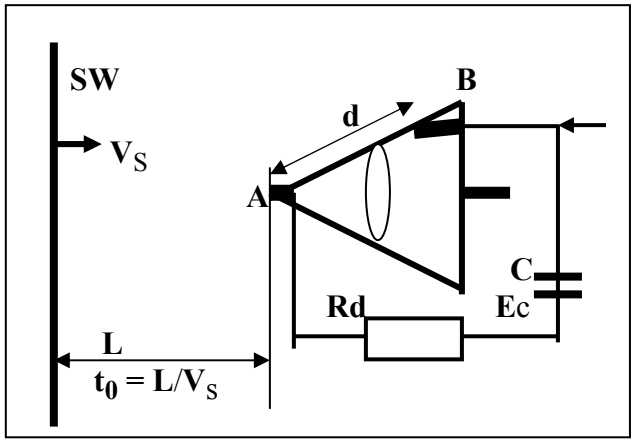

Figure1. Schematic of the problem

Experimental installation.

The experiments are carried in a shock tube (described previously [6,7]), including experimental section with optical windows and cone with apex half-angle of 24° and base diameter of 40 mm. The cone was in site of view of the shadow device TE-19. The cone contained two electrodes, one – on the cone apex,

second - at back part face. Gap length between electrodes was 40 mm, electrodes area - 0,1cm^2. The schematic of the discharge circuits is shown on figure 2.

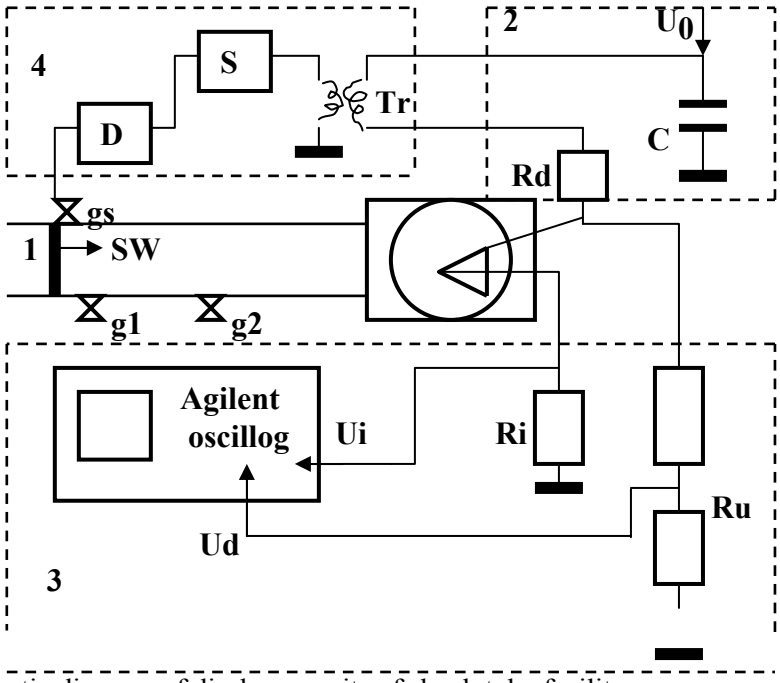

Figure 2. Schematic diagram of discharge units of shock tube facility.

On the Figure3: **1** – shock tube in which shock wave **SW** propagates from left to right (M=2.2-2.5) in air at initial pressure of 20Torr, piezogauges **g1** and **g2** are used for shock velocity measurement, and **g3** – for discharge start. Unit **2** is power discharge source, containing high voltage generator and part of discharge circuit with accumulating discharge capacitor **C** = 4μf, pulse starting transformer winding **Tr** and resistance **Rd**=1kOhm. The voltage $\mathbf{U_0}$ close to a breakdown that (1.7 – 2.0 kV) was constantly put to a discharge gap. In the unit **3** the discharge parameters measured by oscilloscope Agilent-54624A recording the oscillograms of discharge voltage on the resistance **Ru**=100Ohm, and discharge current on the resistance **Ri**=0.36Ohm. The unit **4** is setup of synchronization and discharge starting, it contain delay generator **D**, which drives discharge starting time and so allowed to control the energy input value, and equipment **S**, which form discharge start signal. The Discharge was initiated by a signal from a shock wave for (0.3 – 2.6)ms before shock arrival to cone apex. The passage of a shock inside the gas discharge region along a cone surface was accompanied by failure of the gas discharge. The photo of the discharge area is submitted on Figure 3 in absence of a shock wave for a provisional estimation of the area energy input sizes by a seen part of the discharge, which was about 4cm^3

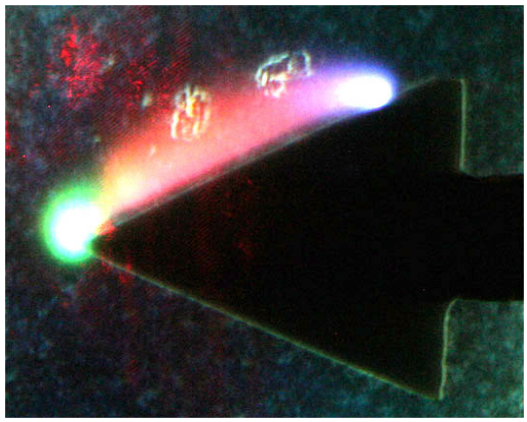

Figure 3. Image of gas discharge without a shock.

The examples of a temporary course of a voltage and a discharge current received from oscillograms are submitted on figure 4. for maximal discharge duration. The top curve (**U**, kV) - change of a voltage on a

discharge gap. During the discharge, the voltage falls from initial $\mathbf{U_0}$ down to (0.2 – 0.4)kV, the voltage grows after termination of the discharge up to size appropriate to a charge, stayed on discharge capacity **C**. The growth of a current up to the maximum in the discharge beginning (1.3-1.5)A (and appropriate power failure) occurred in time about 10μs.

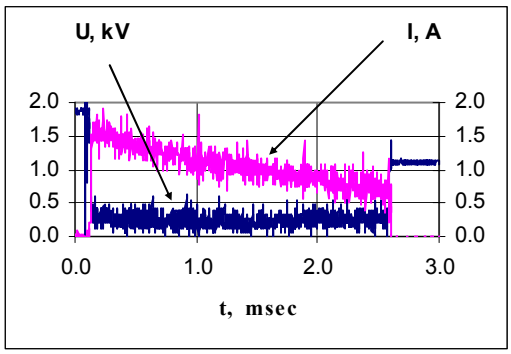

Figure 4. Time variation of a voltage **U** (kV) on a discharge gap (top oscillogram) and the discharge current **I** (A) (bottom oscillogram) with growth up to size (1.3-1.5)A in the discharge beginning.

The discharge duration $\mathbf{t_0}$ (determining energy input values) was determined from oscillograms. Common specific energy input in the discharge area basically depending on the discharge duration was in an interval (0.1 – 0.01)J/cm^3. Average current density on electrodes was (11 – 14)A/cm^2. The discharge voltage during the gas discharge remained poorly varied, however from experience to experience changed on value in an interval 200-400V.

Results.

In the absence of gas discharge one can see the ordinary Mach configuration, that scheme presented on figure 5.

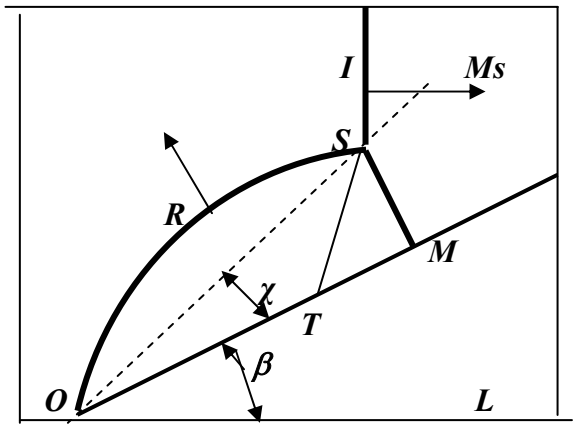

Figure 5. Schematic diagram of Mach configuration on a cone.

Here ***OL*** –cone axis, ***LOM*** - cone apex half-angle (β=24˚), ***OM*** - reflecting surface of a cone, ***IS*** - the part of an incident shock wave, propagating with Mach number M_S, ***RS*** - reflected shock, ***SM*** – Mach stem, ***ST*** - contact surface, ***OS*** - trajectory of triple-point ***S***, χ - angle of triple-point trajectory on a reflecting surface.

The evolution of process of shock interaction with a cone at the plasma formation in the discharge region is visible on Figure 6, 7 and 8. As the plasma formation of the discharge reaches to some extent and ahead a cone, the perturbation of a significant part of incident shock front is observed already right at the beginning of cone-shock interaction.

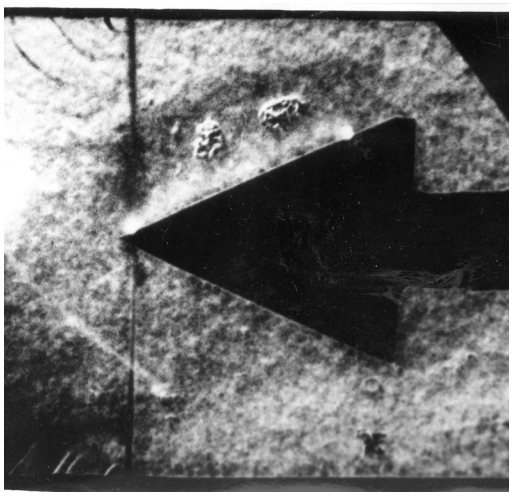

Figure 6. A beginning of a shock-cone-discharge region interaction.

On Figure 6 interaction of a shock (M=2.40) on a cone at discharge duration $\mathbf{t_0}$=1.45ms is submitted. Here it is visible, that the entrance of the incident shock in the discharge region was accompanied by formation of the significant disturbed part of the front: the top point of the disturbed part of incident front follows a border of some area connected to the discharge. It is not caused by acoustic disturbance by the discharge in view of the rather long duration of the discharge.

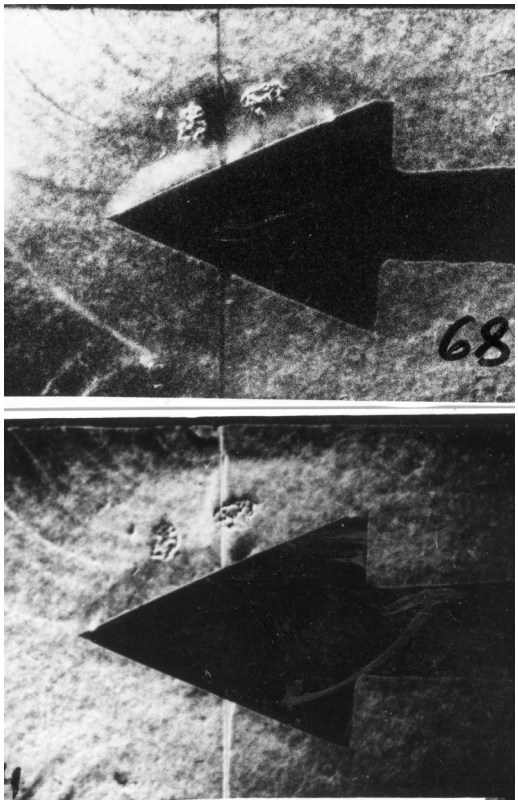

Figure 7. Schlieren-photos of shock passage in the central part of the discharge region for various adjustments of the shadow device

During the propagation of a shock along the cone surface, the discharge is broken. It is evident from voltage and discharge current oscillograms on figure 4.
As it is visible from figure 7, in the top part of the cone in rather cold incoming gas the head shock wave is formed. In the bottom part of the cone the head wave is poorly distinct because of shadow device knife setting. On the figure 7 the pictures of flow are submitted for two knife position: when the knife of the shadow device blocks the light areas of a positive or negative density gradient.

At the further propagation of a shock wave at the exit from the discharge region (figure 8), the front of the disturbed part of the incident shock is more precisely formed as a result of the shock propagation in area with a positive density gradient and negative temperature gradient. It is accompanied by growth of parameters at the front waves and, hence, of more precise visualization of density jump. This front in a much more measure, than usual Mach stem, is advanced and departs from the surface of the cone.

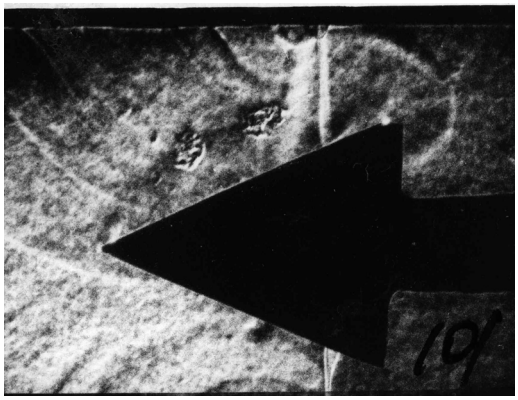

Figure 8. Formation of shock front near to the exit from the discharge area.

It is necessary to note, that in the research of reflection of a shock from a wedge with the discharge [7] the close picture (Figure 9) was received, also corresponding to the exit from the discharge area.

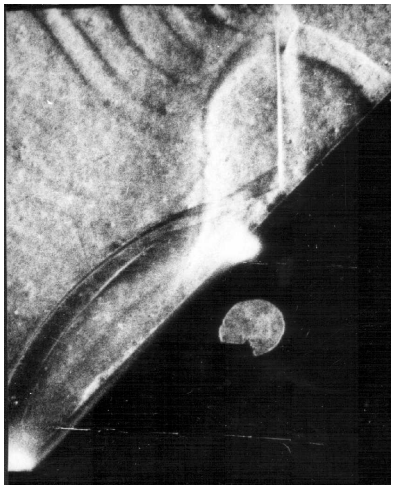

Figure 9. Mach reflection from a wedge 45º with the discharge occupying the bottom part of a inclined wedge reflecting surface.

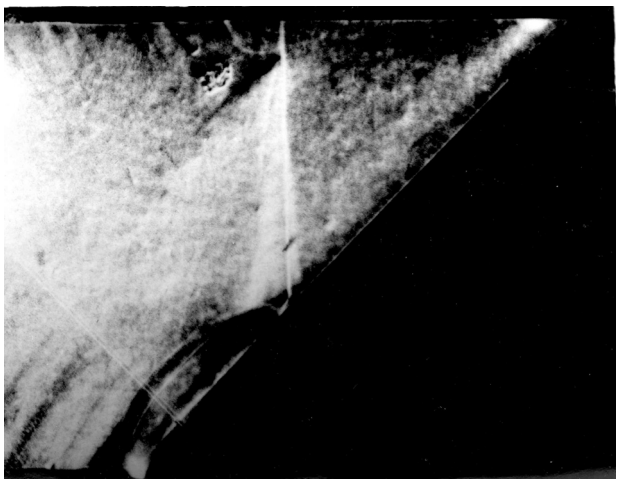

Figure 10. Perturbation of shock front at the discharge expanding all length of a wedge 45º. Near to the basis of a shock front here is an ordinary Mach reflection.

As the discharge occupies only a part of a wedge reflecting surface, here it is registered also the usual Mach reflection near to the wedge surface. The large-scale perturbation formed above and after exit from discharge area. Later on, the pictures of wave interaction with a wedge were received in the discharge region proper. One is submitted on Figure 10, where we see, that, as well as on a cone, the perturbation on incident front is propagated to significant distance from a reflecting wedge surface. The discharge was realized here on full length of a wedge from apex up to the wedge top. As well as on a cone on Figure 10, the contact surface is going here downwards from the top disturbed point on incident front and separated more dense gas behind.

For the quantitative description of process of interaction, the flow scheme considered on Figure 11. The shock wave SW, propagating from left to right, it is submitted in three consecutive positions at interaction with a cone with a discharge close to upper part of the cone. The bow shock wave in the bottom part is not shown.

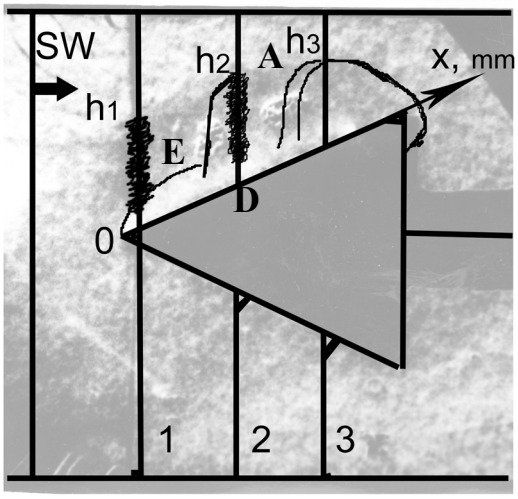

Figure 11. Shock-cone with gas discharge area interaction pattern.

Position of a point **A**, being disturbing shock front, defined as height **h**, where **h** is a distance from the top line of a cone (point **D**). Position of the front is defined by coordinate **x** (point **D**) from the cone apex. Height **h** of the disturbed part of front depending on **x** (excepting an initial site) is submitted on figure 12. It is visible, that it remains (on the average) constant, that is the limit of disturbance of shock front approximately is parallel to line of a cone.

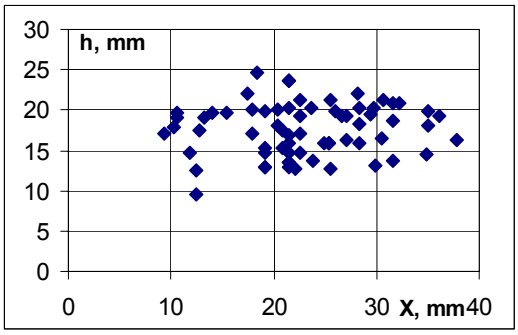

Figure 12. Dependence of height of the shock disturbed part from the position of the shock on the cone.

On figure 13 the values of **h/x** from **x** is submitted, grouping according intervals of value of **x**. The disorder in each group of points is possible because of various values of energy input.

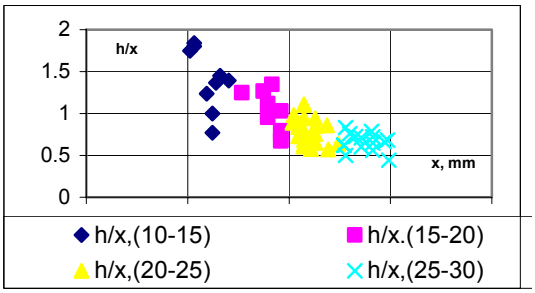

Figure 13. Dependence of the grouped values of reduced height **h/x** for the disturbed zone as the function of the shock position **x** on the cone.

On Figure 14 and Figure 15 the dependences **h/x** as the function of the discharge duration (energy input duration **t** ms) for shock waves which are taking place in an interval of values $10 < x < 15$ (mm) and $15 < x < 20$ (mm), accordingly are submitted.

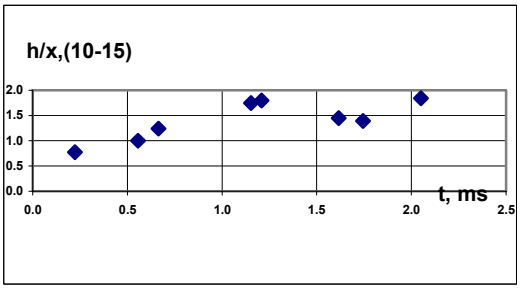

Figure 14. Reduced height of the disturbed part of shock front **h/x** as the function of the discharge duration **t** for shock located in an interval $10 < x < 15$mm.

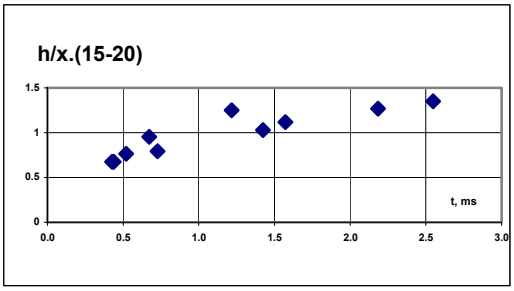

Figure 15. Reduced height of the disturbed part of shock front **h/x** as the function of the discharge duration **t** for shock located in an interval 15 < x < 20mm.

The increase of this size with growth of energy input duration is visible from the diagrams. The finding - out of the reasons of this growth demands detailed consideration of processes in plasma formation of the gas discharge. The consideration of dependence **h/x** from energy input, probably, is advisable by the study of the disorder of the received energy input from duration of the discharge. This disorder is demonstrated on figure 16, where the dependence of energy input value in the discharge area as the function of the discharge duration is submitted.

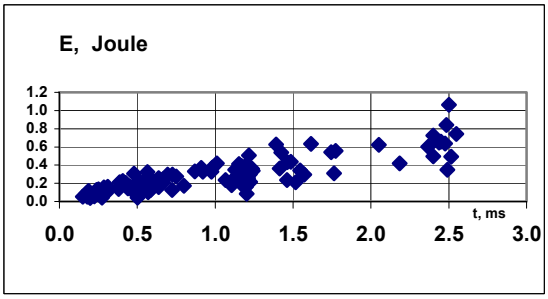

Figure 16. The energy input in discharge area as the function of the discharge duration.

The further propagation of the shock wave (situation 3 in a Figure 11) and the exit from discharge area is accompanied by formation of complex shock configuration, which front essentially outstrips incident front. However, experiments on a wedge [7], our experiments yet have not answered while a question - as far as the arisen configuration has peripheral character of the discharge. The obtained shock configuration seems to be similar to three-dimensional λ–shock studied in work [8] experimentally and in work [9] numerically

The conclusion

The new type of a configuration is found out connected with incidence of a shock on a cone with discharge area near reflecting surface. For more detailed revealing of a nature of this phenomenon the further research both nature of the discharge, and geometry of a configuration is necessary.

Acknowledgment

This work was supported by RFBR under Grant 03-01-00730 and by the Program of the Presidium of the Russian Academy of Sciences “Interaction of Plasma with High-Speed Gas Flow”.

References

[1] Chernyi GG (1998) The Impact of Electromagnetic Energy Addition to Air Near the Flying Body on Its Aerodynamic Characteristics. Proc. 2nd WIG Workshop, Norfolk, VA, pp. 1-31
[2] Chernyi G (1999) Some Recent Results in Aerodynamic Applications of Flows with Localized Energy Addition. Proc 3rd AIAA WIG Workshop, Norfolk, VA, AIAA Paper1999-4819, pp.1–19

[3] Yan H, Adelgren R, Elliott G, Knight D, Beutner T (2003) Effect of energy addition on MR – RR transition. Shock Waves, v.13, pp. 113-121
[4] Adelgren R, Yan H, Elliott G, Knight D, Beutner T, Zheltovodov A, Ivanov M, Khotyanovsky D (2003) Localized Flow Control by Laser Energy Deposition Applied to Edney IV Shock Impingement and Intersecting Shocks. AIAA-2003-0031, 41st Aerospace Sciences Meeting and Exhibit, 6-9 Jan 2003, Reno, Nevada, pp. 1-37
[5] Levin V, Afonina N, Gromov V, Georgievsky P, Terentjeva L (1998) Influence of Energy Input by Electric Discharge on Supersonic Flows Around Bodies. 2ndWeakly Ionized Gases Workshop, AIAA, Norfolk, Virginia USA, pp. 201-231
[6] Fokeev VP, Grin YuI, Levin VA, Sharov YuL (2002) About Some Peculiarities of Mach Configuration Entry to the Discharge Region. In Bityurin VA (ed) The Fourth Workshop on Magneto-Plasma Aerodynamics for Aerospace Applications, Moscow, IVTAN, pp. 297-301
[7] Fokeev VP, Grin YuI, Levin VA, Sharov YuL, Tunik YuV (2003) The influence of Gas Discharge on Propagation of Triple-Shock Mach Configuration – Numerical and Experimental Investigations. In Bityurin VA (ed) The Fifth Workshop on Magneto-and Plasma Aerodynamics for Aerospace Applications, Moscow, IVTAN, pp. 234-239
[8] Bityurin VA, Klimov AI, Leonov SB, Fokeev VP, Kharitonov AI (2000) The Experimental Research of Plane Shock Wave Propagation in Plasma of Transverse-Pulsing Discharge. In Bityurin VA (ed) The 2-nd Workshop on Magneto-Plasma-Aerodynamics in Aerospace Applications, IVTAN, Moscow, pp. 275-278
[9] Bityurin VA, Lutsky AE (2000) Numerical Simulation of 3D Shock Wave Interaction with Thermal Discontinuities In Bityurin VA (ed) The 2-nd Workshop on Magneto-Plasma-Aerodynamics in Aerospace Applications, IVTAN, Moscow, pp. 279-285